Mechanical and Electrical Relaxation in ThO_2 Containing CaO

J. B. WACHTMAN, JR.*
National Bureau of Standards, Washington, D. C.
(Received 27 February 1963)

The dynamic behavior of oxygen vacancies associated with the solid solution of CaO in ThO_2 is treated using an 8-position nearest neighbor model. This treatment predicts an internal friction peak characterized by a single relaxation time and a dielectric loss peak with a single relaxation time equal to twice the mechanical relaxation time. Both peaks have been observed and are in accord with these predictions within experimental error. The activation energy for the motion of an oxygen vacancy neighboring a substitutional Ca ion in 98.5 ThO_2+1.5 CaO is 0.93±0.02 eV.

INTRODUCTION

THIS paper consists of two parts. First, the theory of the mechanical and dielectric effects resulting from the motion of oxygen vacancies around an impurity atom is worked out for an eight-position (cubic) model. Second, data are presented for ThO_2 containing small amounts of CaO and the results are shown to be in agreement with theoretical predictions where comparison is possible. The Ca atoms are assumed to enter the ThO_2 structure (the cubic, fluorite structure in which each Th atom has eight nearest neighbor oxygen atoms) by replacing Th atoms with the formation of an equal number of oxygen vacancies. An approximate calculation indicates that each vacancy is so tightly bound to a Ca ion that to a good approximation it can occupy only the eight nearest neighbor oxygen positions moving from one to another so that each is occupied with equal probability in the absence of stress or electric field; mechanical and dielectric effects arise from partially ordered distributions caused by applied fields.

Breckenridge[1] was apparently the first to state that both mechanical and dielectric effects could result from the motion of a vacancy trapped by an impurity atom. He visualized various detailed possibilities, but his mathematical treatment was based on a two-position model and will not be used here. Hoffman[2] and various collaborators have treated dielectric effects using mathematically similar many-position models for the rotation of a polar molecule; a representative list of publications is given in a survey paper by Hoffman.[3] The present work has much in common with Hoffman's work, but differs in that mechanical effects are also treated, in the inclusion of driving terms in the rate equations, and in the use of group theory to classify relaxation modes. Lidiard[4] included driving terms in the rate equations to treat electrical effects for a particular model, but did not use the concept of relaxation modes. Haven and van Santen[5,6] have used group theory to classify relaxation modes for problems of this type, but they do not show what connection exists between their modes and the rate equations, i.e., no proof is given that their relaxation modes are modes in the sense of being solutions of the rate equations including driving terms. A very abstract discussion of the use of group theory in classifying relaxation phenomena is given by Falk and Meixner.[7]

It has thus been realized for some time that it would be interesting to measure both mechanical and electrical properties on the same material to see if the relaxation times are in the ratio given by the appropriate relaxation modes. Dreyfus[8] has reported electrical measurements on NaCl doped with various impurities including Cd and Sr. Laibowitz and Dreyfus[9] indicate agreement with the prediction of Haven and van Santen[6] for the model appropriate to the anelastic loss in NaCl doped with Cd and Sr. Related discussions of the interpretation of electrical and mechanical losses have been given by Dreyfus and Nowick[10] and by Nowick and Heller.[11] The writer gave a preliminary report[12] of the present work indicating the existence of related mechanical and electrical effects in ThO_2 doped with CaO.

I. THEORY OF MECHANICAL AND ELECTRICAL RELAXATION

1. Rate Equations

In this section, the rate equations, including driving terms, will be derived. These equations relate the occupation probabilities of oxygen vacancies on various oxygen sites to the change in the corresponding potential energies caused by application of stress or electric field. The eventual goal is to obtain expressions for the effect

* This work is based on a thesis submitted in partial fulfillment of the requirements for the degree of Doctor of Philosophy at the University of Maryland, College Park, Maryland.

[1] R. G. Breckenridge, J. Chem. Phys. **16**, 959 (1948); **18**, 913 (1950); in *Imperfections in Nearly Perfect Crystals*, edited by W. Shockley, W. H. Hollomon, R. Maurer, and F. Seitz (John Wiley & Sons, Inc., 1954), p. 219.

[2] J. D. Hoffman, J. Chem. Phys. **20**, 541 (1952).

[3] J. D. Hoffman, Arch. Sci. Geneva **12**, 37 (1959).

[4] A. B. Lidiard, in *Report on the Conference on Defects in Crystalline Solids* (The Physical Society, London, 1954), p. 283.

[5] Y. Haven and J. H. van Santen, J. Chem. Phys. **22**, 1146 (1954).

[6] Y. Haven and J. H. van Santen, Suppl. Nuovo Cimento **7**, 605 (1958).

[7] G. Falk and J. Meixner, Z. Naturforsch. **11a**, 728 (1956).

[8] R. W. Dreyfus, Phys. Rev. **121**, 1675 (1961).

[9] R. B. Laibowitz and R. W. Dreyfus, Bull. Am. Phys. Soc. **7**, 224 (1962).

[10] R. W. Dreyfus and A. S. Nowick, J. Appl. Phys. **33**, 473 (1962).

[11] A. S. Nowick and W. R. Heller, Bull. Am. Phys. Soc. **7**, 224 (1962).

[12] J. B. Wachtman, Jr., Bull. Am. Ceram. Soc. **40**, 187 (1961).

of oxygen vacancy motion upon the elastic moduli and the internal friction and upon their electrical analogs, the dielectric constant and dissipation factor. This goal is approached in the following steps: (a) The solution of the rate equation is shown to depend on the solution of the eigenvalue problem for a matrix occurring in the rate equations, (b) The eigenvectors of this matrix are shown to be related to the basis vectors of the irreducible representations of the point group for a symmetrical set of wells and barriers, (c) The potential energy changes are written as a linear function of stress or electric field, and (d) Expressions are then derived for the mechanical and electrical properties of interest. The 8-position model will be used as a specific example throughout the development, but much of the treatment will be more general. Some detailed manipulations are omitted; these can be found in the writer's thesis.[13]

The numbering of the sites which a given oxygen vacancy can occupy is arbitrary, but must be chosen and kept fixed; the numbering chosen for the 8-position model is shown in Fig. 1. The crystal axes x, y, z are shown with a substitutional Ca atom at the origin and the eight neighboring oxygen sites numbered as shown. For any other substitutional Ca atom, the crystal axes are to be translated without rotation and the sites numbered in the same way. The occupation number N_β of oxygen vacancies on sites with position β is defined by

$$N_\beta=\sum_{\alpha=1}^{N^c} O_{\alpha\beta} \tag{1}$$

where N^c is the number of substitutional Ca atoms and $O_{\alpha\beta}$ is the number of vacancies on sites of type β for the αth Ca atom. Assuming all the oxygen vacancies neighbor Ca atoms and that there is one oxygen vacancy per Ca atom, one has

$$\sum_{\beta=1}^{8} N_\beta=N^c. \tag{2}$$

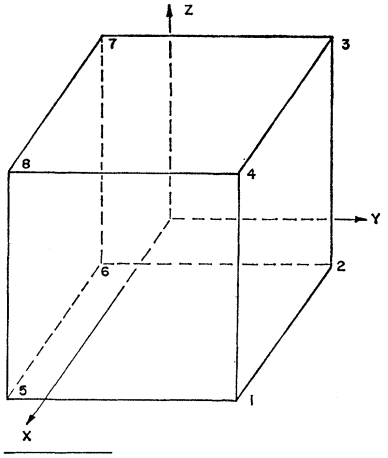

FIG. 1. The numbering used for the sites of the 8-position mode.

[13] J. B. Wachtman, Jr., Ph.D. Thesis, University of Maryland, 1961 (unpublished); available University microfilms, order number 61-6254.

In the absence of any perturbing effect, such as stress or electric field, there should be no preference for any type of site and N_β will have the value $N^c/8$ for each value of β. This will no longer be true when the system is perturbed; n_β is introduced as a measure of the deviation from randomness and is defined by

$$n_\beta=N_\beta-N^c/8. \tag{3}$$

The frequency with which an oxygen vacancy jumps from the β to the γ oxygen site is defined to be $W_{\beta\gamma}$ and is taken to be zero except for jumps between neighboring sites; all nonzero $W_{\beta\gamma}$ have the value W in the absence of any perturbing force. The jump frequency is assumed to be thermally activated with activation energy E so that

$$W=W_0\exp(-E/kT)=W_0\exp(-R/T), \tag{4}$$

where k is Boltzmann's constant, T is the absolute temperature, $R=E/k$, and W_0 is the limiting frequency. The action of a small perturbing force is assumed to affect the jump frequency $W_{\beta\gamma}$ by the change in the activation energy resulting from the increase u_β in the potential energy of the β position and the increase $u_{\beta\gamma}$ in the potential energy at the saddle point in going from the β to the γ site. The rate equation for site one is

$$dN_1/dt=-N_1(W_{12}+W_{14}+W_{15})+N_2W_{21}+N_4W_{41}+N_5W_{51}. \tag{5}$$

Assuming $u_\beta-u_{\beta\gamma}\ll kT$ gives

$$W_{\beta\gamma}=W\left(1+\frac{u_\beta-u_{\beta\gamma}}{kT}\right) \tag{6}$$

for the nonzero $W_{\beta\gamma}$ and substituting for N_β gives

$$dN_1/dt+W(3n_1-n_2-n_4-n_5)=-(WN^c/8kT)(3u_1-u_2-u_4-u_5)+(WN^c/8kT)\times[(u_{12}-u_{21})+(u_{14}-u_{41})+(u_{15}-u_{51})], \tag{7}$$

where only first-order terms in small quantities have been kept. In a first approximation, the oxygen vacancy may be pictured as moving on a potential-energy surface which depends on the crystal and any externally applied field, but which does not depend on the position of the vacancy itself. One then has $u_{\beta\gamma}=u_{\gamma\beta}$ and the last term in Eq. (7) vanishes. The potential-energy surface may, however, depend on the position of the vacancy in the following sense. The vacancy will induce a polarization in the surrounding crystal which will interact with the vacancy and contribute to the potential energy. If a vacancy crosses a saddle point more rapidly than this polarization can relax, the energy at the saddle point may depend on the direction of the jump, i.e., $u_{\beta\gamma}\neq u_{\gamma\beta}$. The inclusion of such polarization effects greatly complicates the problem. Ninomiya[14] has treated polarization effects for complexes in a twelve-position model for a special case which reduces to a three-position model. He finds

[14] T. Ninomaya, J. Phys. Soc. Japan 14, 30 (1959).

that the dielectric relaxation is still characterized by a Debye-type curve but that the amplitude of the dielectric loss is changed. Fuchs and von Hipple[15] have shown that polarization effects in a two-position model can lead to a spectrum of relaxation times as well as a change of amplitude. We recognize that such polarization effects may be important in some cases, but we shall assume $u_{\beta\gamma}=u_{\gamma\beta}$ and proceed. Our justification is that we wish to treat those aspects of the problem related to the symmetry of the 8-position model, and that our experimental data fit the resulting equation.

The whole set of eight rate equations for the eight sites can then be written in matrix form as

$$\left(\mathbf{I}\frac{1}{W}\frac{d}{dt}+\mathbf{C}\right)\mathbf{n}=-\frac{N^c}{8kT}\mathbf{C}\mathbf{u}, \tag{8}$$

where $\mathbf{I}$ is the unit matrix of degree eight, $\mathbf{n}$ is the single-column eight-row matrix of n_β, and $\mathbf{u}$ is the single-column eight-row matrix of u_β. The matrix $\mathbf{C}$ for the 8-position model numbering the sites as shown in Fig. 1 has the value

$$\mathbf{C}=\begin{vmatrix} 3 & -1 & 0 & -1 & -1 & 0 & 0 & 0 \\ -1 & 3 & -1 & 0 & 0 & -1 & 0 & 0 \\ 0 & -1 & 3 & -1 & 0 & 0 & -1 & 0 \\ -1 & 0 & -1 & 3 & 0 & 0 & 0 & -1 \\ -1 & 0 & 0 & 0 & 3 & -1 & 0 & -1 \\ 0 & -1 & 0 & 0 & -1 & 3 & -1 & 0 \\ 0 & 0 & -1 & 0 & 0 & -1 & 3 & -1 \\ 0 & 0 & 0 & -1 & -1 & 0 & -1 & 3 \end{vmatrix}.$$

For a more general model of Z equivalent neighboring sites, $\mathbf{C}$ is a square matrix of degree Z with each diagonal element equal to the number of nearest neighbor potential wells and with -1 in each row at the position corresponding to a nearest neighbor for that row number. The matrix form of the rate equation for Z wells is

$$\left(\mathbf{I}\frac{1}{W}\frac{d}{dt}+\mathbf{C}\right)\mathbf{n}=-\frac{N^c}{Zkt}\mathbf{C}\mathbf{u}, \tag{9}$$

where $\mathbf{n}$ and $\mathbf{u}$ now have Z rows and $\mathbf{C}$ has degree Z. Note that $\mathbf{C}$ is real and symmetric so that eigenvectors corresponding to discrete eigenvalues are orthogonal.

2. Relaxation Modes

We now show that the eigenvectors of C are relaxation modes of Eq. (9). Assume that the eigenvalues, λ_γ, and the eigenvectors, $\mathbf{l}_\gamma$ have been found. The effect of a sinusoidal variation of a stress or electric field will be to cause sinusoidal variations of the u_β. The resulting $\mathbf{u}$ can be expressed in terms of the eigenvectors of $\mathbf{C}$ by writing

$$\mathbf{u}=\sum_{\gamma=1}^{Z} a_\gamma\mathbf{l}_\gamma\exp(j\omega_\gamma t), \tag{10}$$

where a_γ is a time-independent expansion coefficient, ω_γ is the angular frequency, and $j=\sqrt{-1}$. This expansion is always possible; Parter[16] has shown that the eigenvectors of a matrix with the properties of $\mathbf{C}$ form a complete set (i.e., span the column space of $\mathbf{C}$). We look for a solution of the form

$$\mathbf{n}=\sum_{\gamma=1}^{Z} b_\gamma\mathbf{l}_\gamma\exp(j\omega_\gamma t+\phi_\gamma), \tag{11}$$

where b_γ is a time-independent expansion coefficient and ϕ_γ is a phase angle. Substituting into (9) and using the orthogonality of the eigenvectors of $\mathbf{C}$, we obtain

$$\tan\phi_\gamma=-\omega_\gamma/\lambda_\gamma W \tag{12}$$

and

$$b_\gamma=-(a_\gamma N^c/ZkT)[1+(\omega_\gamma/\lambda_\gamma W)^2]^{-1/2}. \tag{13}$$

In practice, we shall be most concerned with the case in which both the $\mathbf{u}$ and the $\mathbf{n}$ expansions contain only the eigenvectors corresponding to strain or electric field as will be discussed in Sec. I4.

3. Use of Group Theory in Classifying Relaxation Modes

We now show that the relaxation modes form bases of irreducible representations of the point group of the set of sites by showing that the matrix $\mathbf{C}$ commutes with the matrix representing any of the point group operations in a given representation. The representation most useful for our purposes is given by a group of permutation matrices of degree Z. Each of the set of equivalent sites is represented by a single-column Z-rowed matrix composed of zeros except for a one in the row whose number is equal to the number of the site. A given symmetry operation of the point group is represented by a permutation matrix which takes these column matrices into each other in the same way that the symmetry operation transforms sites into each other. The set of all these permutation matrices forms a matrix group which we call the immediate representation of the point group and which is unique for a given numbering of the sites. Let $\mathbf{P}$ be a matrix of this group. Multiplying both sides of Eq. (9) by $\mathbf{P}$ gives

$$\left(\mathbf{I}\frac{1}{W}\frac{d}{dt}+\mathbf{C}'\right)\mathbf{n}'=-\frac{N^c}{ZkT}\mathbf{C}'\mathbf{u}', \tag{14}$$

where

$$\mathbf{C}'=\mathbf{P}\mathbf{C}\mathbf{P}^{-1}, \tag{15}$$

$$\mathbf{n}'=\mathbf{P}\mathbf{n}, \tag{16}$$

and

$$\mathbf{u}'=\mathbf{P}\mathbf{u}. \tag{17}$$

Now the effect of $\mathbf{P}$ is just to change the numbering of the sites. Equation (14) is the rate equation for the same set of sites which have just been renumbered. This re-

[15] R. Fuchs and A. von Hipple, J. Chem. Phys. **34**, 2165 (1961).

[16] S. Parter, J. Soc. Ind. Appl. Math. **8**, 376 (1960).

numbering is not arbitrary because nearest neighbors must remain nearest neighbors under point group operations. Consider the element $\mathbf{C}_{\beta\gamma}'(\beta\neq\gamma)$ of $\mathbf{C}'$ and suppose that sites β and γ (in the new numbering) are nearest neighbors so $\mathbf{C}_{\beta\gamma}'=-1$. The sites β and γ in the old numbering are obtained by $\mathbf{P}^{-1}$ which preserves the nearest neighbor relationship so that $\mathbf{C}_{\beta\gamma}=-1$ also. If elements β and γ (in the new numbering) are not nearest neighbors, then $\mathbf{C}_{\beta\gamma}'=0$ and, by the same argument, $\mathbf{C}_{\beta\gamma}=0$. The diagonal elements of $\mathbf{C}$ are all equal and the effect of $\mathbf{P}$ is just to rearrange them. Thus, the corresponding elements of $\mathbf{C}'$ and $\mathbf{C}$ are equal so that $\mathbf{C}'=\mathbf{C}$ and we have the result that $\mathbf{C}$ commutes with any element $\mathbf{P}$ of the immediate representation. We can now use the results of representation theory for the eigenvalues of a matrix, $\mathbf{C}$, which is invariant under a group. The necessary results are worked out in detail by Lomont[17] in the context of molecular vibrations, but the results are quite general. The important result is based on Schur's lemma and states that the representation, Γ, of a group under which $\mathbf{C}$ is invariant can be written as a direct sum of irreducible representations, Γ_P, and that the matrix $\mathbf{C}$ can be written as a corresponding direct sum of submatrices of degree equal to the degree of each of the irreducible representations appearing in Γ. This means that the secular equation of $\mathbf{C}$ will factor into parts corresponding to each of the Γ_P appearing in Γ. Furthermore, the theory shows that all of the eigenvalues corresponding to one Γ_P are equal and that the corresponding eigenvectors form a basis for that Γ_P. The representation Γ can be written as a direct sum,

$$\Gamma=\sum_{P=1}^{r} C^P\Gamma_P. \tag{18}$$

The integral coefficients, C^P, can be calculated[17] from

$$C^P=\frac{1}{g}\sum_{i=1}^{r} r_i\chi_i^{(P)*}\chi_i, \tag{19}$$

where g is the order of the group, i designates the class, r is the number of the classes, r_i is the number of group elements of the ith class, $\chi_i^{(P)}$ is the trace of the ith class in the Pth irreducible representation, χ_i is the trace of the ith class in the representation Γ, and * indicates complex conjugate. In the present application, one obtains r_i and $\chi_i^{(P)}$ from the character table for the point group; χ_i is simply the number of sites left unmoved (mapped onto themselves) by any operation of the ith class. The latter statement follows from the fact that in a permutation matrix the diagonal elements are zero except that those which correspond to no change are equal to one.

For the 8-position model considered here, the appropriate point group is O_h, the full cubic group, whose character table is given by Koster.[18] When the above calculations are carried out, one obtains for Eq. (18)

$$\Gamma=\Gamma_1+\Gamma_2'+\Gamma_{25}'+\Gamma_{15}, \tag{20}$$

where Koster's notation for the irreducible representations is used. The basis function for Γ_1 transforms like $x^2+y^2+z^2$ which gives the eigenvector $\mathbf{l}_1$, with eigenvalue zero, shown in Fig. 2. The basis function for Γ_2' transforms like xyz, which gives the eigenvector $\mathbf{l}_2$ with eigenvalue 6. The basis functions for Γ_{25}' transform like xy, yz, and zx, which give the eigenvectors $\mathbf{l}_3$, $\mathbf{l}_4$, and $\mathbf{l}_5$, which have the common eigenvalue 4. The basis functions for Γ_{15} transform like x, y, and z, which give the eigenvectors $\mathbf{l}_6$, $\mathbf{l}_7$, and $\mathbf{l}_8$, with common eigenvalue 2.

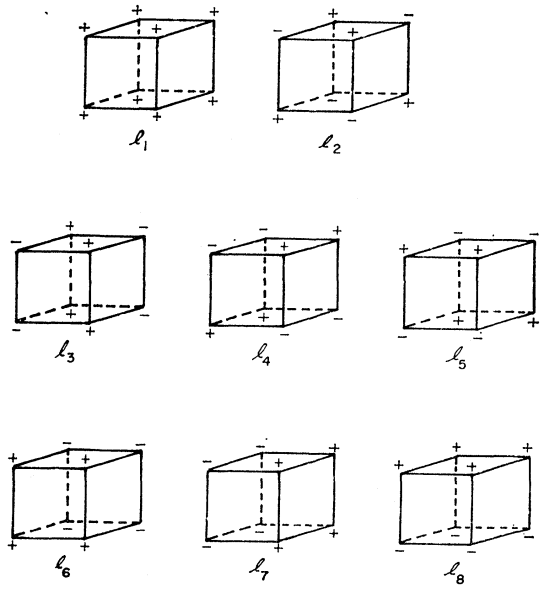

FIG. 2. Eigenvectors (relaxation modes) for the 8-position model.

4. Relation of Energy Variable to Stress and Electric Field

When an electric field, E, is acting, the energy difference between any two sites is proportional to the field. Taking a^e as the constant of proportionality, the general result is

$$\mathbf{u}=a^e(E_x\mathbf{l}_6+E_y\mathbf{l}_7+E_z\mathbf{l}_8). \tag{21}$$

The physical significance of a^e is that it is equal to half the dipole-moment change caused by a single-vacancy jump if E_x, E_y, and E_z are taken as components of the local field. We could take this moment to be the change (which raises the question of the degree of ionic character) times the distance moved. Our experimental results, however, do not permit a check of the size of the dipole moment because of uncertainty about the number

[17] J. H. Lomont, *Applications of Finite Groups* (Academic Press Inc., New York, 1959), pp. 102–109.

[18] G. F. Koster, in *Solid State Physics*, edited by F. Seitz and D. Turnbull (Academic Press Inc., New York, 1957), Vol. 5, p. 174.

of vacancies; therefore, we keep a^e as a parameter to be determined by curve fitting. This permits us to take E_x, E_y, and E_z as components of the external field and absorb the uncertainty about the local field into a^e. The dipole moment per unit volume, $P_x{}^c$, resulting from n vacancies jumping in volume v will be

$$P_x{}^c=2na^e/v. \tag{22}$$

A stress which has only tensile components when referred to the crystal axes (such as a tensile stress along [100]) causes no difference in the potential energy of the vacancies on different sites. This can be seen by noting that there is no relaxation mode with the symmetry of a tensile stress. The mechanical modes $\mathbf{l}_3$, $\mathbf{l}_4$, $\mathbf{l}_5$, are active under shear stress, σ_{12}, etc., and the resulting energy change is

$$\mathbf{u}=a^\sigma(\sigma_{12}\mathbf{l}_3+\sigma_{23}\mathbf{l}_4+\sigma_{13}\mathbf{l}_5). \tag{23}$$

The meaning of a^σ can be seen by considering the effect of a stress σ_{13} applied suddenly. In addition to the instantaneous elastic strain not related to vacancy motion, there will be an additional strain, $\epsilon_{13}{}^c$, as n vacancies jump in volume, v, to give a distribution $\mathbf{n}=-(n/4)\mathbf{l}_5$. The energy taken from the stress field by vacancy motion will be

$$2v\sigma_{13}\epsilon_{13}{}^c=-2nu_1. \tag{24}$$

Combining with (23) gives

$$\epsilon_{13}{}^c=-na^\sigma/v. \tag{25}$$

5. Mechanical Properties

The contribution of the stress-driven oxygen vacancy motion to energy dissipation will first be calculated for a single crystal under stress σ_{23}; average over all orientations will then be taken to calculate the internal friction of a polycrystalline specimen in flexure. If the stress acting on a single crystal is $\sigma_{23}{}^0\sin\omega t$, there will be a corresponding elastic strain $\epsilon_{23}=s_{44}\sigma_{23}{}^0\sin\omega t$ where $\sigma_{23}{}^0$ is a constant, stress-amplitude factor and s_{44} is the elastic compliance giving shear strain for unit shear stress. There will be an additional strain component $\epsilon_{23}{}^c=a^\sigma n/v$. Using Eq. (11) for n gives

$$\epsilon_{23}{}^c=\frac{(a^\sigma)^2N^c}{8vkT}\left[\frac{\sin\omega t}{1+(\omega/4W)^2}-\frac{(\omega/4W)\cos\omega t}{1+(\omega/4W)^2}\right]\sigma_{23}{}^0. \tag{26}$$

The in-phase portion contributes to the elastic modulus and for one percent CaO in ThO_2 the contribution is just large enough to be detected. The out-of-phase portion of $\epsilon_{23}{}^c$ contributes to the internal friction, $Q^{-1}=\Delta U/2\pi U$, where U is the vibrational energy and ΔU is the energy dissipated per cycle. The latter is given by

$$\Delta U=2\int_0^{2\pi/\omega}\sigma_{23}\frac{d\epsilon_{23}}{dt}dt. \tag{27}$$

If the specimen is polycrystalline, an applied tensile stress, σ_{11}', acting along an axis x' with direction cosines a_{11}, a_{12}, and a_{13}, to the xyz axes will produce stresses σ_{12}, σ_{13}, and σ_{23}. The resulting energy dissipation calculated from (26) is

$$\Delta U=\frac{(a^\sigma)^2N^c}{4vkT}\frac{\omega/4W}{1+(\omega/4W)^2}(\sigma_{12}{}^2+\sigma_{13}{}^3+\sigma_{23}{}^2); \tag{28}$$

using the tensor transformation law gives

$$\sigma_{12}{}^2+\sigma_{13}{}^2+\sigma_{23}{}^2=[(a_{11}a_{12})^2+(a_{11}a_{31})^2+(a_{21}a_{31})^2+(a_{21}a_{31})^2](\sigma_{11}')^2. \tag{29}$$

If the quantity in brackets is averaged over all orientations, the result is $2/5\pi$. The energy dissipation is thus

$$\Delta U=\frac{(a^\sigma)^2N^c}{10\pi vkT}\left[\frac{\omega/4W}{1+(\omega/4W)^2}\right](\sigma_{11}')^2. \tag{30}$$

If Y is the Young's modulus of the polycrystalline specimen, the stored energy is

$$U=(\sigma_{11}')^2/2Y. \tag{31}$$

Using (30) and (31) gives

$$TQ^{-1}=\frac{Y(a^\sigma)^2N^c}{10\pi^2vk}\left[\frac{\omega/4W}{1+(\omega/4W)^2}\right]. \tag{32}$$

Using (4) and letting

$$A=Y(a^\sigma)^2N^c/20\pi^2vk \quad\text{and}\quad S=\ln(\omega/4W_0)$$

gives

$$TQ^{-1}=A\,\mathrm{sech}(S+R/T). \tag{33}$$

6. Electrical Properties

The contribution of the electrically driven oxygen vacancy motion to the energy dissipation is closely analogous to the result for the mechanical case. An electric field, $E_x=E_x{}^0\sin\omega t$, will cause a polarization $P_x{}^0$ plus a contribution $P_x{}^c$ resulting from reorientation of the oxygen vacancy–calcium ion pairs. Using Eq. (22) for $P_x{}^c$ and Eq. (11) for n gives

$$P_x{}^c=\frac{(a^e)^2N^c}{4vkT}\left[\frac{\sin\omega t}{1+(\omega/2W)^2}-\frac{(\omega/2W)\cos\omega t}{1+(\omega/2W)^2}\right](E_x{}^0)^2. \tag{34}$$

The out-of-phase portion of $P_x{}^c$ contributes to the dissipation factor, $D=\Delta U/2\pi U$, where ΔU and U have the same meaning as before except that now the driving force is electric field rather than stress. The energy dissipation will be made up of a part due to the motion of pairs which can be calculated in the same way as the mechanical loss plus a part due to the electrical conductivity. Letting D_c represent the contribution to the dissipation factor from this conductivity, one obtains in

place of (32) the result

$$T(D-D_c)=\frac{(a^e)^2N^c}{Kvk}\frac{\omega/2W}{1+(\omega/2W)^2}, \quad (35)$$

where K is the dielectric constant. Using (4) and letting $A'=(a^e)^2N^c/2Kvk$ and $S'=\ln(\omega/2W_0)$, one obtains in place of (33) the result

$$T(D-D_c)=A'\,\mathrm{sech}(S'+R/T). \quad (36)$$

Note that no distinction has been made between single crystals and polycrystalline specimens in the case of the dielectric properties because ThO_2, being cubic, should be isotropic with respect to dielectric constant and electrical conductivity.

II. EXPERIMENTAL RESULTS

1. Applicability of 8-Position Model to ThO_2 Containing CaO

ThO_2 is known to accept CaO in solid solution up to 12.5 mole%; the lattice parameter remains unchanged and this, together with evidence from sintering rates, suggests that Ca substitutes for Th with the formation of one oxygen vacancy per calcium atom.[19] The electrostatic attraction between an oxygen vacancy (effective charge $2eq_1$) and a substitutional calcium ion (effective charge $-2eq_2$) should cause association. Using Pauling's[20] electronegativity scale gives $q_1=0.70$ and $q_2=0.79$ and taking the static dielectric constant to be 18.4 gives a difference of electrostatic energy of 0.34 eV between nearest neighbor and next-nearest neighbor positions. The degree of association can be calculated following the lines of a statistical calculation by Lidiard.[21] The degree of association should be least for low concentrations of CaO and high temperatures. For the lowest concentration (0.4% CaO) and highest temperature (600°K) used in the present work, the resulting[13] degree of association is 99.2%; at lower temperatures or higher concentrations, the degree of association should be even closer to 100%. The electrostatic energy and the statistical calculation are both approximate, but the results do make it reasonable to assume 100% association.

A substitutional Ca ion can jump to an equivalent position only by interchanging with a Th ion. An oxygen vacancy, however, can move from one to another of the eight oxygen sites neighboring the substitutional Ca ion by the jump of a single oxygen ion and this seems a more probable process. Thus, the model of a fixed Ca ion with an oxygen vacancy jumping by single steps over the eight oxygen positions neighboring the Ca ion seems reasonable.

2. Preparation of Specimens

The high melting point of ThO_2, usually taken[22] as 3300°C, makes the growing of large single crystals by existing techniques very difficult and limits the practical possibilities to the use of sintered polycrystalline specimens. Powder mixtures were made from ThO_2 obtained from the Lindsay Chemical Company and with Baker's reagent grade calcium carbonate. The latter was used instead of calcium oxide because of the general experience that calcium oxide freshly formed by calcining calcium carbonate is more reactive than calcium oxide which has been standing for some time. The powder was pressed without binder into bars in a rectangular steel mold using a pressure of 2000 psi. Each bar was then sealed in a rubber bag and repressed isostatically in water to 30 000 psi. All bars were sintered in one heating of a large gas-fired furnace which was brought up to 1800°C over a period of a day, kept at 1800°C for 1 h, and cooled over a 2-day period. Compositions included nominally pure ThO_2 and ThO_2 with CaO in these molar percentages: 0.4, 1.0, and 1.5. Spectroscopic analysis showed the principal impurities in the nominally pure ThO_2 to be Al, Mg, and Si in the range 0.01 to 0.1%.

Initial measurements of the variation of mechanical and electrical properties were made on roughly machined bars. This was possible because, as shown in the next section, the physical properties of interest can be expressed as ratios which do not involve the dimensions of the specimens to first order. A procedure for accurate machining was eventually worked out (involving diamond grinding of 0.0005 in. per pass) and absolute values were measured at 25°C using accurately ground bars (for Young's modulus) and disks or rectangular slices (for the dielectric constant).

3. Experimental Technique

Values of Young's modulus and the internal friction were determined by Förster's method,[23] in which a bar is suspended horizontally from two fine threads (Fiberglas threads were used in the present work) and vibrated in flexure by driving the upper end of one thread. The other thread is attached to a crystal pickup. The procedure for determining the resonance frequencies and for calculating the absolute values of elastic moduli has recently been discussed[24] very fully. The result for Young's modulus is

$$Y=0.94642\rho l^4f^2T_1/t^2, \quad (37)$$

where ρ is the density, l is the length, f is the flexural resonance frequency, t is the thickness in the direction of vibration, and T_1 is a correction factor which is very close to 1.00 and whose value can be determined.[24] The

[19] J. R. Johnson and C. E. Curtis, J. Am. Ceram. Soc. **37**, 611 (1954); C. E. Curtis and J. R. Johnson, *ibid.* **40**, 63 (1957).
[20] L. Pauling, *The Nature of the Chemical Bond* (Cornell University Press, Ithaca, New York, 1960), 3rd ed.
[21] A. B. Lidiard, Phys. Rev. **94**, 29 (1954).
[22] E. Ryschkewitch, *Oxide Ceramics* (Academic Press Inc., New York, 1960).
[23] F. Forster, Z. Metallk. **29**, 109 (1937).
[24] S. Spinner and W. E. Tefft, Proc. Am. Soc. Testing Materials **61**, 1221 (1961).

value of Y at some temperature T can be expressed in terms of its value at the reference temperature of 25°C with an accuracy probably better than 1 in 10^4 by

$$Y(T)=Y(25)\left[\frac{f(i)}{f(25)}\right]^2\frac{l(25)}{l(T)}. \tag{38}$$

The thermal expansion of ThO_2 has been determined[25] so that only the resonant frequency need be measured to obtain the variation of $Y(T)/Y(25)$ with temperature. The internal friction can be calculated from

$$Q^{-1}=\frac{\ln(A_0/A_1)}{\pi f\Delta t}, \tag{39}$$

where A_0 and A_1 are the amplitudes of vibration at the beginning and end of an interval, Δt, of undriven, freely decaying vibration. In practice, the supporting threads contribute to the damping[26] and a compromise must be made between placing the threads near the nodes of vibration (small thread contribution to damping but small signal) and far from the nodes (large signal but large damping by the threads). For the ThO_2 bars used in the present work, a satisfactory compromise was accomplished by tying the threads a fraction 0.167 of the length from the ends (the nodes are 0.224 from the ends). The specimens were lowered into place on the axis of a specially wound horizontal tube furnace through a slot which was then packed with insulation except for two openings for the threads. Measurements were made in air. The frequency was determined with an accuracy of ± 0.1 cps with a crystal-controlled frequency counter. The decay pattern was recorded by shutting off the drive and simultaneously triggering a storage oscilloscope. The amplitudes A_0 and A_1 and the time interval Δt were read from the resulting pattern.

The capacitance and dissipation factor values for flat plates or disks were determined by two-terminal measurements with a General Radio 716-C bridge using the substitution method. The method has been fully described.[27] Platinum electrodes were applied using a commercial platinum paint at room temperature and heating to 600°C. Measurements were made in a vertical tube furnace with the specimen lying on a $\frac{1}{4}$-in.-thick platinum disk in the center of the furnace which served as the ungrounded electrode contact. The ground electrode contact was provided by one side of a platinum-platinum 10% rhodium thermocouple which was held in an alumina insulating tube on the axis of the furnace above the specimen. This insulating tube was clamped outside the furnace in a metal sleeve which was free to move vertically. Thus, the weight of the tube and sleeve pressed the thermocouple bead against the upper electrode of the specimen; a bridge balance and temperature reading were made with the bead in this position. A bridge balance with the circuit broken at the specimen, required in the calculations, was obtained by raising the sleeve and, thus, breaking the contact between the bead and the upper specimen electrode.

4. Absolute Values at 25°C

The absolute values are of little concern to the present work and are reported only as incidental results. Young's modulus for a pure ThO_2 bar with density 9.076 g/cm³ was 1.997×10^{12} dyn/cm². This density corresponds to a porosity of 9.2% and the present Young's modulus value falls on a curve of Young's modulus as a function of porosity determined by Spinner, Knudsen, and Stone.[28] For ThO_2 containing 1.5 mole% CaO and having a porosity of 1.3%, the value was 2.380×10^{12} dyn/cm².

The dielectric constant was first determined at 695 cps using two thoria plates. The first gave 16.3 for pure ThO_2 and 17.8 for ThO_2 containing 1.5% CaO. Bottcher[29] has given the following equation for the dielectric constant at zero porosity, K_0, in terms of the value, K, at porosity P:

$$K_0=K\left(\frac{1+2K-3P}{1+2K-3PK}\right). \tag{40}$$

Kerner[30] has independently treated the case of packed grains of different phases and his equation reduces to that of Bottcher for a porous, single-phase material. Use of this equation gives zero porosity values of 18.6 for pure ThO_2 and 18.1 for ThO_2 containing 1.5% CaO. These values are higher than the accepted handbook value of 10.6 for pure ThO_2 determined by Gunther-schultze and Keller[31] at 2×10^6 cps. These investigators used the method of liquid-powder mixtures which can give a low value if entrapped air is not eliminated. The difficulty is illustrated by the work of Nagasawa[32] who found a value of 3.2 for pure ThO_2 using the method of mixtures. To check the present work, a disk of pure ThO_2 with porosity 8.7% was very carefully ground and measured twice, first with tin foil electrodes pressed on with vaseline and then with fired-on platinum electrodes. The former gave a K value of 16.2 and the latter 15.7; these values were independent of frequency over the range of measurement, 10^2 to 10^6 cps. The value of 15.7 may be low because of the vaseline film; the value of 16.2 gives a calculated value of 18.4 for ThO_2 with zero porosity.

---

[25] J. B. Wachtman, Jr., T. G. Scuderi, and G. W. Cleek, J. Am. Ceram. Soc. **45**, 319 (1962).
[26] J. B. Wachtman, Jr., and W. E. Tefft, Rev. Sci. Instr. **29**, 517 (1958).
[27] *American Society of Testing Materials Supplement* (American Society of Testing Materials, Philadelphia, 1954), Part 6, p. 223.
[28] S. Spinner, F. P. Knudsen, and L. Stone, J. Res. Nat. Bur. Std. **67C**, 39 (1963).
[29] C. J. F. Bottcher, *Theory of Electric Polarization* (Elsevier Publishing Company, Inc., Amsterdam, 1952).
[30] E. H. Kerner, Proc. Phys. Soc. (London) **B69**, 802 (1956).
[31] A. Guntherschultze and F. Keller, Z. Physik **75**, 78 (1932).
[32] W. Nagasawa, J. Electrochem. Soc. Japan **18**, 158 (1950).

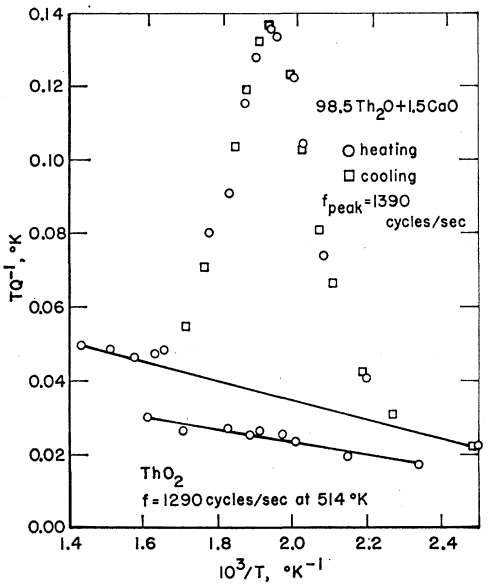

FIG. 3. Product of internal friction and absolute temperature (including background) for pure ThO_2 and for 98.5 ThO_2+1.5 CaO as a function of reciprocal absolute temperature.

5. Temperature Dependence of Measured Properties

The experimental results for the internal friction, Q^{-1}, are shown in Fig. 3 as a plot of TQ^{-1} as a function of T^{-1} for comparison with Eq. (33). The plot for thoria containing 1.5% CaO shows a well-defined peak. Measurements on pure ThO_2 were made carefully to lower the background contribution from the supporting threads as much as possible; the resulting plot for pure ThO_2 still probably reflects loss in the threads and loss by radiation of sound rather than internal friction in the specimen, but it shows that the peak occurring in the CaO-doped specimen is absent. These results suggest that this background loss can best be represented by straight lines as drawn on the plot. Figure 4 shows the data for 98.5 ThO_2+1.5CaO after this estimated background loss has been subtracted. Equation (33) was fitted to these data by using a technique of expanding the hyperbolic secant around approximate initial values of R and S, using the least squares criterion to obtain corrections to R and S, and repeating to converge on the final values which are given in Table I together with the activation energy $R/k=0.93$ eV. It can be seen that Eq. (33) fits the data. From Eq. (26), we see that there should be a corresponding contribution to the strain and, hence, a corresponding reduction in the measured elastic modulus as the temperature is increased through the region of the internal friction peak. Figure 5 shows that there does appear to be a reduction in Young's modulus over the right temperature range, but that it is small and is superimposed on the normal decrease in Young's modulus (characteristic of pure thoria[33]) so that

[33] J. B. Wachtman, Jr., W. E. Tefft, D. G. Lam, Jr., and C. S. Apstein, Phys. Rev. 122, 1754 (1961).

TABLE I. Results of internal friction measurements on thoria specimens with varying CaO content.

Mole % CaO	0.4	1.0	1.5
Frequency at peak cps	1152	1501	1390
A (°K)	0.054±0.001	0.098±0.002	0.101±0.001
R (10^3 °K)	11.8 ±3	11.0 ±0.3	10.8 ±0.2
E (eV)	1.02 ±0.03	0.95 ±0.03	0.93 ±0.02
S	−23.0 ±0.6	−21.3 ±0.5	−21.4 ±0.4
Peak temperature (°K)	514.3	515.0	514.5
W_0 (10^{13}/sec)	1.99	0.32	0.31
ν (10^{13}/sec)	0.63	0.60	0.60
$\exp(\Delta S/R_0)$	3.02	0.54	0.54
Wert-Zener range of $\exp(\Delta S/R_0)$	1 to 5	1 to 4	1 to 4

no curve fitting can be attempted. The mechanical resonance frequency at the peak in Fig. 4 was 1390 cps and Eq. (36) shows that if an electrical experiment were run at half this frequency (to make $S'=S$) a peak in the loss would be expected. The dissipation factor was measured at 695 cps for both pure ThO_2 and 98.5 ThO_2+1.5 CaO. The curve for the latter shows a plateau in the loss followed by a steep rise with increasing temperature, but the pure ThO_2 shows only a smooth rise. It was assumed that at high temperature in the doped thoria the loss was by volume conductivity which was assumed to vary exponentially with reciprocal temperature. The high-temperature data were used to obtain

$$D_C=20.3-12.4\times10^3T^{-1} \qquad (41)$$

as an estimate of dissipation factor due to this mechanism in the doped thoria. Using this equation, the line

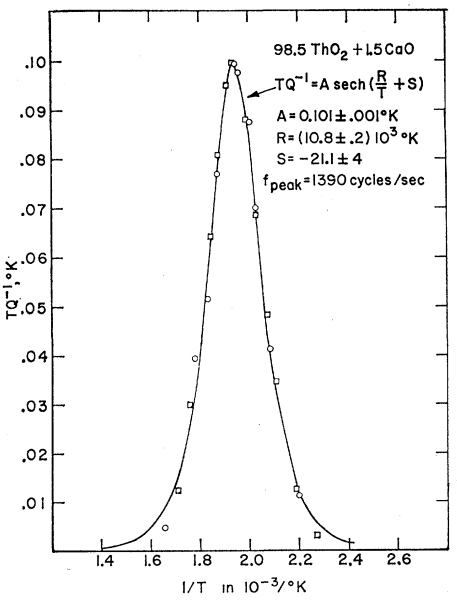

FIG. 4. Product of internal friction and absolute temperature (with background subtracted) for 98.5 ThO_2+1.5 CaO as a function of reciprocal absolute temperature.

plotted in Fig. 6 for doped thoria was drawn and the difference values between the observed points and this line were attributed to the effect of the CaO doping. These difference points are shown in Fig. 7. The parameters obtained from the internal friction data (shown on Fig. 4) can be used in Eq. (36) to give all but the parameter A'. The latter was chosen to make the height of the curve drawn in Fig. 6 fit the experimental points; the temperature of the peak and its width are determined by R and S (i.e., from the internal friction data) and agree with the experimental points. The ratio of capacitance at temperature T to capacitance at 25°C is shown for both pure and doped thoria at 695 cps in Fig. 8. The pure thoria shows a smooth rise with increasing temperature which may be a space-charge effect. The doped

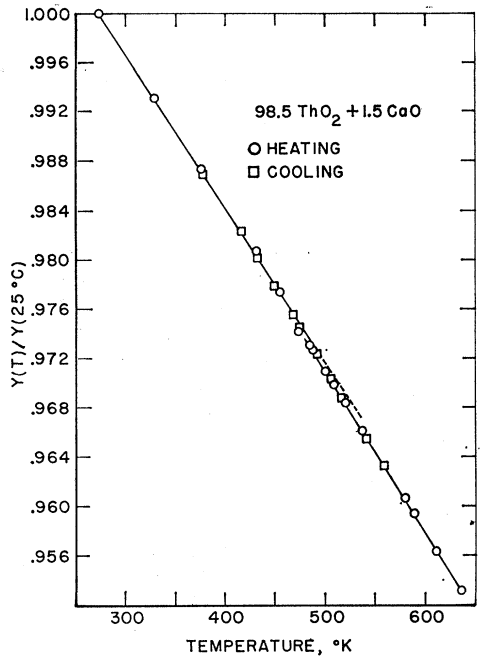

FIG. 5. Young's modulus ratio for 98.5 ThO_2+1.5 CaO as a function of temperature.

thoria shows a bend in the curve, suggesting that there is a contribution from the CaO superimposed upon the smooth rise found for pure ThO_2. The contribution of the calcium ion-oxygen vacancy pairs can be calculated from the in-phase part of Eq. (34). The resulting equation for $K(T)/K(25)$ is shown on Fig. 8 and the function is plotted for comparison with the data. It appears reasonable that the curve for doped thoria is made up of a smooth background effect (as in pure thoria) plus a contribution as shown by the curve for $K(T)/K(25)$, but a quantitative statement cannot be made because of lack of knowledge concerning the background effect.

The effect of a shift in frequency of electrical measurement should simply be to change S' by an amount which can be calculated. In Fig. 9, measurements made

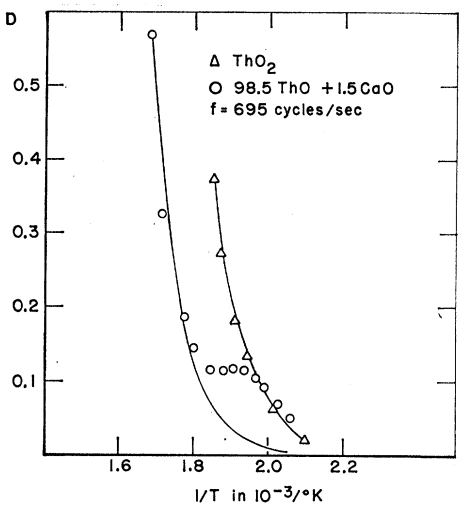

FIG. 6. Dissipation factor (including background) for pure ThO_2 and for 98.5 ThO_2+1.5 CaO as a function of reciprocal absolute temperature.

at 6950 cps are compared with the sech plotted using the calculated value of S'.

Internal friction measurements were also made on specimens with 0.4 and with 1.0 mole% CaO. The results are summarized in Table I. In each case, the data (corrected for background loss) could be fitted by Eq. (33) using the parameters in Table I.

6. Discussion

The predictions of the theory for which the present data provide a check are as follows:

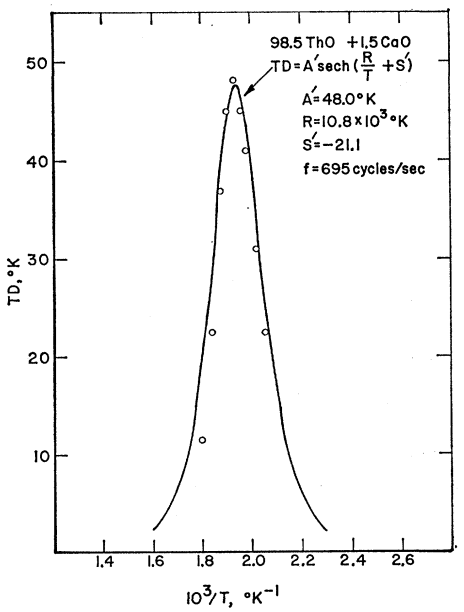

FIG. 7. Product of dissipation factor and absolute temperature for 98.5 ThO_2+1.5 CaO as a function of reciprocal absolute temperature at 695 cps.

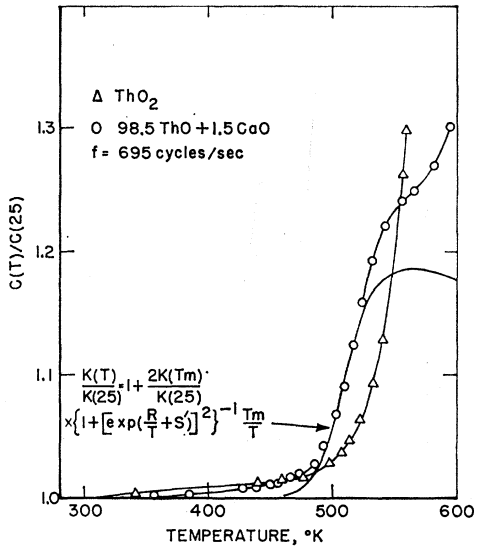

FIG. 8. Capacitance ratio for pure ThO_2 and for 98.5 ThO_2+1.5 CaO as a function of temperature.

First, there should be an internal friction peak and a dielectric loss peak, which are absent in pure ThO_2 and which increase in height with increasing CaO content. This is confirmed except that the peak for 1.5% is not significantly larger than that for 1.0% CaO as the A values of Table I indicate. Perhaps some clustering of pairs to form quadrapoles or other motionless clusters occurs at high CaO concentration.

Second, each peak should be characterized by a single relaxation time; the good fit of the hyperbolic secant to the data confirms this.

Third, the electrical relaxation time should be twice the mechanical relaxation time; this appears to be true because the peak in the dielectric loss occurs at the same temperature as the internal friction peak when the electrical measurements are made at half the frequency of the mechanical measurements. The uncertainty in the peak temperature is about $\pm 3°$, which is equivalent to about 12% uncertainty in the relaxation time ratio; within this uncertainty, the ratio of observed relaxation times appears to be two. Strictly, the theory gives the ratio of the microscopic relaxation time (for an isolated pair), but the experiment was done under conditions where the interaction of pairs could cause a local field effect which can cause the observed macroscopic relaxation time to differ from the microscopic relaxation time. Powles[34] has proposed an equation relating the two times; use of his equation leads to a prediction that the ratio of the observed electrical to mechanical relaxation time should be 2.14, which is still within the estimated 12% uncertainty.

The mean time of stay for any one of the three oxygen atoms which can change place with a bound oxygen vacancy is equal to $1/W_0$, the pre-exponential factor in the treatment of reaction-rate theory given by Wert and Zener.[35,36] This is equal to the product of a jump frequency ν and an entropy factor $\exp(\Delta S/k)$ were ΔS is the activation entropy. They estimate ν from

$$\nu = (E/2m\lambda^2)^{1/2}, \tag{42}$$

where λ is the distance between oxygen positions in our application. The values of ν and $\exp(\Delta S/k)$ given in Table I were calculated in this summer. Wert and Zener argue that $\exp(\Delta S/k)$ cannot be less than one and they give an approximate upper limit in terms of the slope of the elastic modulus-temperature curve. The values of $\exp(\Delta S/K)$ for 1.0 and 1.5% CaO doping lie below the Wert-Zener range, but the accuracy of W_0 and of the method of estimating from Eq. (42) is not good enough to be certain that this difference is significant.

A prediction of the theory which cannot be checked on polycrystalline specimens is the result that the mechanical modes are active under shear, but not under tensile strain, along one of the cube axes. A polycrystalline bar with tensile strain along the bar axis will contain many grains having a nonzero component of shear strain in the crystal axes of the grain and this is presumably the reason why the internal friction peak could be observed in the present experiment. It would be a crucial test of the present 8-position model to measure internal friction in tension (which should not give a peak) and shear (which should give a peak) on a CaO-doped thoria single crystal, but a large enough crystal is not yet available.

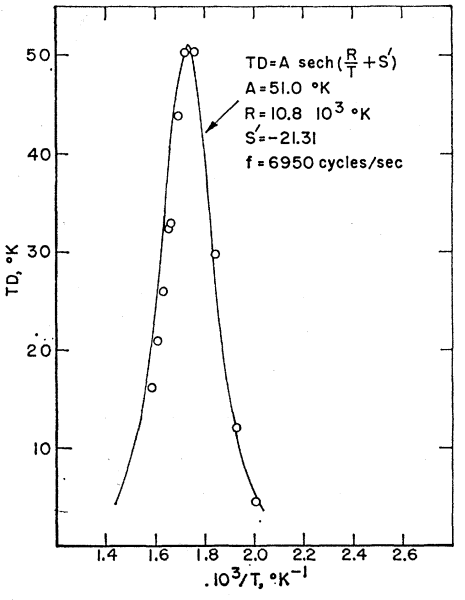

FIG. 9. Product of dissipation factor and absolute temperature for 98.5 ThO_2+1.5 CaO as a function of reciprocal temperature at 6950 cps.

[34] J. G. Powles, J. Chem. Phys. **21**, 633 (1953).

[35] C. Wert and C. Zener, Phys. Rev. **76**, 1169 (1949).

[36] C. Wert, Phys. Rev. **79**, 601 (1950).

The coefficient of T^{-1} in Eq. (41) gives an activation energy of 1.04 eV for the volume electrical conductivity in thoria doped with 1.5% CaO. This is only slightly larger than the value of 0.93 eV for the motion of an oxygen vacancy neighboring a Ca ion and the activation energy of free oxygen-vacancy motion might well be slightly larger than for the motion of an oxygen vacancy neighboring a foreign ion. The writer originally believed[13] that the volume electrical conductivity could be attributed to oxygen vacancies with an activation energy for motion alone because the number of oxygen vacancies is fixed by the CaO content. Franklin[37] pointed out that while the total number of oxygen vacancies is presumably fixed by the CaO content, most of these are bound to Ca ions and so do not contribute to volume conductivity. The number of free oxygen vacancies should still be thermally activated and conductivity by oxygen-vacancy motion should still require an activation energy which is the sum of an energy of motion and one half the energy of dissociation. The activation energy of 1.04 eV for the volume conductivity compared with 0.93 eV for the pivoting motion of a bound vacancy leaves 0.22 eV for the dissociation energy. As noted previously, an electrostatic calculation indicates that 0.34 eV is the energy difference between a nearest and next-nearest site for an oxygen vacancy. In the same way, we estimate that to completely free an oxygen vacancy from a calcium ion would require 0.71 eV. This is larger than 0.22 eV and the results, therefore, argue against ionic conductivity as the dominant mechanism of electrical conductivity at 500°K but the uncertainty in the electrostatic method of estimating dissociation energy is so great that little weight can be attached to this conclusion.

Two of the specimens prepared for the present work were subsequently studied by Carter,[38] who measured the cell voltage developed by pure ThO_2 between atmospheres of CO_2 and O_2; the results indicate that over the temperature range 750 to 1125°C, the conductivity is primarily electronic. Measurements of the resistivity of 90 ThO_2+10 CaO showed an increase by a factor of 2 or more in going from an O_2 atmosphere to a water-saturated H_2 atmosphere, indicating appreciable electronic conductivity. The slope of the curve for an O_2 atmosphere gave an activation energy of 1.0 eV in close agreement with the value of 1.04 obtained in the present work from the background loss in 98.5 ThO_2+1.5 CaO.

An incidental observation worthy of note is the fact, shown in Fig. 5, that the background loss in 98.5 ThO_2+1.5 CaO is considerably lower than in ThO_2 at the same temperature. Further study of the mechanism of electrical conductivity in pure and doped ThO_2 would be interesting as well as the proposed internal friction measurements if suitable single crystals become available.

ACKNOWLEDGMENTS

The writer acknowledges with pleasure the guidance of his thesis advisor, C. M. Herzfeld. Thanks are gratefully tendered to A. D. Franklin and J. D. Hoffman of the National Bureau of Standards for helpful discussion, and to R. E. Carter of the General Electric Research Laboratory for permission to quote his unpublished results.

[37] A. D. Franklin, National Bureau of Standards (private communication).

[38] R. E. Carter, General Electric Research Laboratory (private communication).